PROCEEDINGS OF THE ROYAL SOCIETY B

Proc. R. Soc. B (2011) **278**, 519–525
doi:10.1098/rspb.2010.1093
Published online 1 September 2010

On optimal hierarchy of load-bearing biological materials

Zuoqi Zhang[1], Yong-Wei Zhang[1] and Huajian Gao[2,*]

[1]*Institute of High Performance Computing, A*STAR, Singapore 138632, Singapore*
[2]*Division of Engineering, Brown University, Providence, RI 02912, USA*

Load-bearing biological materials such as shell, mineralized tendon and bone exhibit two to seven levels of structural hierarchy based on constituent materials (biominerals and proteins) of relatively poor mechanical properties. A key question that remains unanswered is what determines the number of hierarchical levels in these materials. Here we develop a quasi-self-similar hierarchical model to show that, depending on the mineral content, there exists an optimal level of structural hierarchy for maximal toughness of biocomposites. The predicted optimal levels of hierarchy and cooperative deformation across multiple structural levels are in excellent agreement with experimental observations.

Keywords: biomechanics; hierarchical material; quasi-self-similar; biomimetic; toughness; flaw tolerance

1. INTRODUCTION

Multi-level structural hierarchy, as can be observed in a wide range of systems from chromosome, protein, cell, tissue to organisms, seems to be a universal strategy selected by natural evolution for realizing various properties and functions [1–5]. Based on biominerals and proteins (mainly type I collagen), a variety of load-bearing biological materials, such as bone, tooth, shell, tendon and antler, have emerged from evolution with ordered hierarchical microstructures that current man-made materials cannot achieve, and with strength and toughness surpassing their constituent phases by orders of magnitude [6–9]. Much progress has been made over the past several decades on the structure–property relations of biological materials at nano-, micro- and macro-levels, as well as a number of hierarchical levels integrated together [10–12]. In spite of these developments, important questions remain unanswered: what determines the size scales and hierarchical levels in a load-bearing biological material? Should there be an optimal number of structural levels in such materials, or is it simply the more levels the better? These questions are of interest not only to biologists but also to materials scientists who have recently synthesized biomimetic materials with microstructures mimicking, and properties exceeding, their natural counterparts [13–15]. To understand the principle of structural hierarchy in load-bearing biological materials, here we develop a quasi-self-similar structure model to show that, depending on the mineral content, there exists an optimal level of structural hierarchy for maximal toughness of hierarchical materials.

Figure 1 shows the hierarchical composite structures of bone, mineralized tendon and shell with different mineral content (45% of volume fraction in bone, 15% in mineralized tendon and 95% in shell; [6–9]). Bone is seen to exhibit seven levels of structural hierarchy [16,17], with striking self-similarity near the bottom levels of hierarchy (figure 1*a*). Mineralized tendon fibres have four levels of hierarchy (figure 1*b*) with highly ordered, self-similar structures at every level [18], while tendon has six levels of hierarchy [19,20]. By contrast, sea shells show 2–3 levels of lamellar structures (figure 1*c*), with different structures at different levels [21].

To obtain a comprehensive understanding of biological materials, it is particularly important to bridge observations and behaviours across several length scales [22]. So far, there have been only limited studies of biological structures from a global hierarchical point of view. For example, it has been shown that the two-scale surface roughness on a lotus leaf can be explained by a size limit owing to static pressure of liquid drops [23], that the three-level hierarchy of alpha-helix-based protein filaments can be attributed to their optimal strength and toughness [24], and that the three-level structural hierarchy on Gecko's feet can be related to a size limit owing to fibre fracture [25]. For load-bearing biological materials, a previously developed self-similar hierarchical model [10,12] failed to explain experimentally measured strain values of bone at different hierarchical levels [11] as well as why these materials typically exhibit two to seven levels of hierarchy depending on the mineral content. Our present model addresses this gap between theory and experiments, and helps to reveal the basic principles of structural hierarchy of load-bearing biological materials.

2. DERIVATION OF MODEL

Here we develop a quasi-self-similar composite model (figure 2) that mimics the bottom levels of hierarchy in load-bearing biological materials (figure 1). In this model, each hierarchical level consists of slender hard inclusions aligned in a parallel staggered pattern in a soft matrix. The structure at the n-th level serves as reinforcing inclusions at the $(n+1)$-th level. Since evolution

* Author for correspondence (huajian_gao@brown.edu).

Electronic supplementary material is available at http://dx.doi.org/10.1098/rspb.2010.1093 or via http://rspb.royalsocietypublishing.org.

Received 22 May 2010
Accepted 10 August 2010

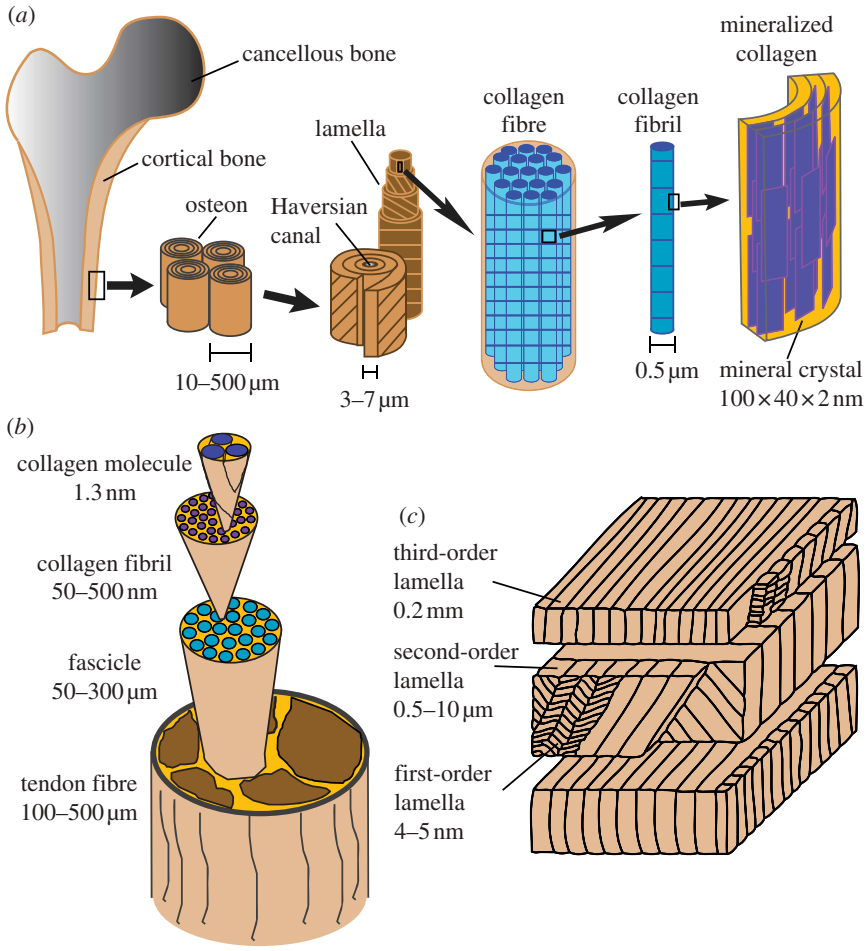

Figure 1. Typical hierarchical structures of load-bearing biological materials: (*a*) bone [7,16], (*b*) mineralized tendon fibre [18], and (*c*) shell [21]. (Figures have been modified based on those from the corresponding papers cited here.)

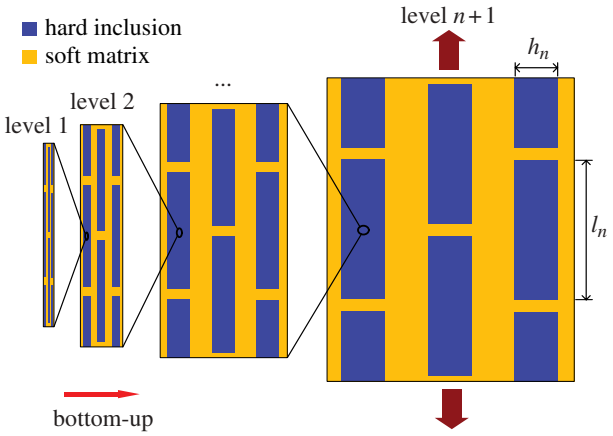

Figure 2. A quasi-self-similar hierarchical material. Every level structure consists of slender hard inclusions (blue) aligned in a parallel staggered pattern in the soft matrix (yellow). The aspect ratio of the inclusions varies from level to level. The inclusions at the $(n+1)$-th level are made of the staggered microstructure at the n-th level.

tends to adapt biological systems to fit their functions, it can be assumed that the hierarchical structures of load-bearing biological materials have been optimized for stiffness and toughness. In accordance with this hypothesis, a set of design principles listed below will be used to construct the quasi-self-similar structural hierarchy and to examine how the material properties vary with the number of hierarchical levels.

(a) *Principle of flaw-tolerance*

In order to maximize toughness, we assume that the hierarchy renders material insensitive to the pre-existing crack-like flaws, a property interpreted as the removal of stress concentration at failure [8]. The condition for hard inclusions at the $(n+1)$-th level of hierarchy to remain flaw-tolerant in the presence of random crack-like flaws is that the characteristic width h_n should satisfy the criterion [10,12,26]

$$h_n \le \frac{E_n \Gamma_n}{S_n^2}, \quad n = 0, 1, 2, \ldots, N, \tag{2.1}$$

where E_n, S_n, Γ_n denote the Young's modulus, strength and fracture energy at the n-th level. The basic material properties at the $n = 0$ level are $E_0 = E_m$, $S_0 = \sigma_m$, $\Gamma_0 = 2\gamma_m$, where E_m, σ_m, γ_m stand for Young's modulus, strength and surface energy of the mineral, respectively. The higher level composite properties ($n = 1, 2, \ldots, N$ level) are calculated by the recursive formulae ([10,12]; also see electronic supplementary material, text A and figure S1)

$$E_n = \left[\frac{4(1-\varphi_{n-1})}{G^p_{n-1}\varphi^2_{n-1}\rho^2_{n-1}} + \frac{1}{\varphi_{n-1}E_{n-1}}\right]^{-1},$$

$$S_n = \frac{1}{2}\varphi_{n-1}\rho_{n-1}\tau^p_{n-1}$$

and $$\Gamma_n = (1-\varphi_{n-1})h_{n-1}\rho_{n-1}\tau^p_{n-1}\Theta^p_{n-1},$$

where φ_{n-1} and ρ_{n-1} represent the volume fraction and aspect ratio of hard inclusions, while G^p_{n-1}, τ^p_{n-1} and Θ^p_{n-1} denote the shear modulus, strength and failure strain of matrix at the n-th level. A related, but slightly different, point of view is that equation (2.1) ensures maximum redundancy of microstructure so that old and damaged materials can be constantly removed and replaced with fresh and healthy materials while an animal is conducting its normal activities [27].

(b) *Criteria of equal strength and efficient stress transfer*

The criterion of equal-strength is to make soft matrix and hard reinforcements reach their corresponding strengths at the same time [8,28]. According to this criterion, the aspect ratio $\rho_n = l_n/h_n$ of hard inclusions at the $(n+1)$-th level is determined as

$$\rho_n^{\mathrm{ESC}} = \frac{S_n}{\tau_n^p}, \quad n = 0, 1, 2, \ldots, N-1, \tag{2.2}$$

where S_n is the tensile strength of the inclusions and τ^p_n is the shear strength of the matrix.

The aspect ratio also plays an important role in the stress transfer between neighbouring inclusions via shear deformation in the matrix. In particular, there exists a critical aspect ratio beyond which a constant shear stress cannot be maintained in the matrix [29–31]. For efficient stress transfer, the aspect ratio should not exceed the following critical value (see appendix A for the derivation),

$$\rho_n^{\mathrm{STC}} = 2\sqrt{\frac{2(1-\varphi_n)E_n}{\varphi_n \tau_n^p/\Theta_n^p}}, \tag{2.3}$$

where τ^p_n and Θ^p_n are, respectively, the shear strength and failure shear strain of the matrix, while E_n and φ_n are Young's modulus and volume fraction of hard inclusions at the $(n+1)$-th level. A combined criterion for selecting the aspect ratio is thus

$$\rho_n = \min\{\rho_n^{\mathrm{ESC}}, \rho_n^{\mathrm{STC}}\}. \tag{2.4}$$

(c) *Limited selection of constituent materials*

Naturally occurring biological materials are constrained by a limited selection of constituent materials available [5,14]. Bone essentially consists of carbonated hydroxyapatite mineral crystals embedded in a soft matrix made of predominantly type I collagen [32,33]. The type I collagen accounts for 85–90% of total protein mass in bone [32]. Based on this fact, we assume that the matrix is made of the same type of protein (i.e. type I collagen) at all hierarchical levels, i.e.

$$\tau_n^p = \tau_p, G_n^p = G_p, \Theta_n^p = \Theta_p, \quad n = 0, 1, 2, \ldots, N-1, \tag{2.5}$$

where τ_p, G_p and Θ_p denote the shear strength, shear modulus and failure shear strain of the soft matrix, respectively. In the electronic supplementary material, text B and figure S2, we will show that this assumption could be relaxed by including two different types of protein without altering the main conclusions of the model.

Constituent materials are distributed at different structural levels in the quasi-self-similar hierarchical material. The volume fraction of mineral, Φ, varies according to the relative importance of stiffness and toughness. Experiments have shown that the stiffness tends to rise while the toughness decreases with increasing mineral content, as in mineralized tendon ($\Phi = 15\%$), bone ($\Phi = 45\%$) and shell ($\Phi = 95\%$) [1,6,7,9,33,34]. This suggests that toughness becomes a more dominant property as the mineral content is reduced. So far, there exists little information on how the constituent materials are distributed at different hierarchical levels. A simplest assumption is that the volume fraction of hard inclusions remains fixed at all hierarchical levels [10,12],

$$\varphi_n = \Phi^{1/N}, \quad n = 0, 1, 2, \ldots, N-1. \tag{2.6}$$

Note that this assumption can also be relaxed without affecting the main conclusions of the model (see electronic supplementary material, text C and figure S3).

The above principles allow the quasi-self-similar hierarchical material to be constructed following a bottom-up design route shown in figure 3. Once the material parameters for mineral and protein, E_m, σ_m, γ_m, τ_p, G_p, Θ_p and Φ, are known, the properties of a N-level hierarchical material can be systematically calculated.

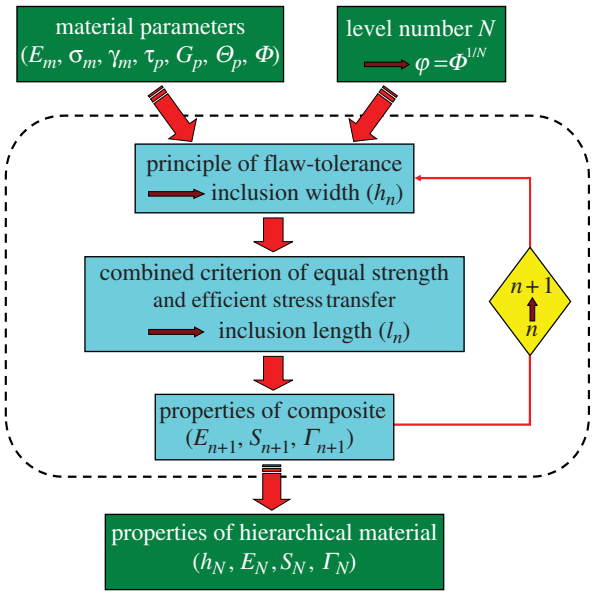

Figure 3. Bottom-up design route for quasi-self-similar hierarchical materials.

3. RESULTS

Figure 4*a–d* plots the calculated properties of the quasi-self-similar hierarchical material as a function of the hierarchical level number N. The results based on the equal-strength criterion are compared with those based on the combined criterion of equal strength and efficient stress transfer. In these calculations, we have taken material parameters to be those of mineralized tendon, $\Phi = 0.15$, $\gamma_m = 1\ \mathrm{J\,m^{-2}}$, $E_m = 100$ GPa, $\sigma_m = E_m/30$, $G_p = E_m/1000$, $\tau_p = \sigma_m/100$ and considered two values $\Theta_p = 35\%$ and $\Theta_p = 100\%$ for the failure shear strain of the matrix. Figure 4*a* plots the overall stiffness of the quasi-self-similar hierarchical material normalized by the Voigt upper bound of the composite. It is seen that the stiffness decreases as the hierarchical level number

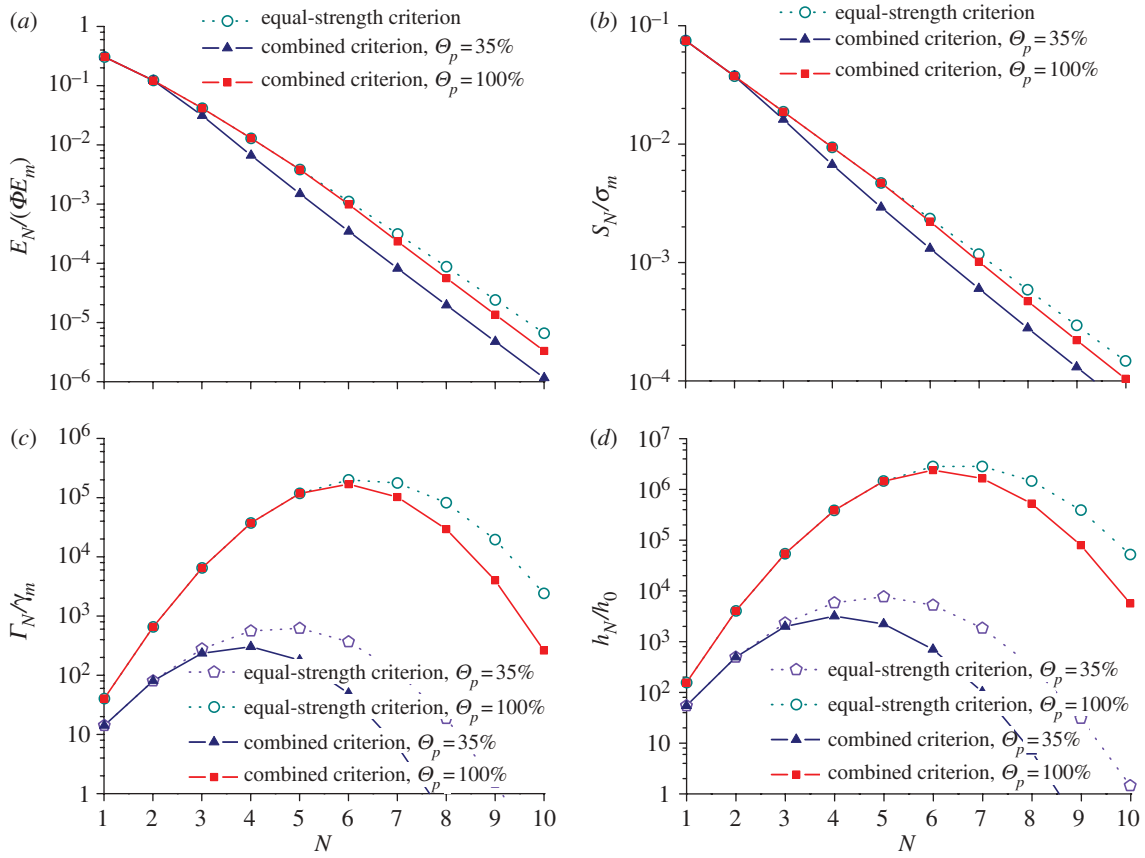

Figure 4. Variations of (*a*) Young's modulus, (*b*) strength, (*c*) toughness, and (*d*) size of an *N*-level quasi-self-similar hierarchical material. (*a*,*b*) Turquoise circles, equal-strength criterion; blue triangles, combined criterion, $\Theta_p = 35\%$; red squares, combined criterion, $\Theta_p = 100\%$. (*c*,*d*) Purple pentagons, equal strength criterion, $\Theta_p = 35\%$; turquoise circles, equal strength criterion, $\Theta_p = 100\%$; blue triangles, combined criterion, $\Theta_p = 35\%$; red squares, combined criterion, $\Theta_p = 100\%$.

N increases. Figure 4*b* shows that the strength of the hierarchical material drops by roughly a factor of 2 with each added level of hierarchy, decreasing by about one order of magnitude with four levels of hierarchy. Figure 4*c* plots the variation of toughness with the hierarchical level number *N* for different Θ_p, showing that the toughness first increases and then decreases with increasing number of hierarchical levels. Therefore, there exists an optimal number of hierarchy for maximum toughness. This optimal number is $N = 4$ for $\Theta_p = 35\%$ and $N = 6$ for $\Theta_p = 100\%$, suggesting that the property of soft material plays an important role in determining the optimal number of hierarchical levels. Interestingly, the plots calculated from the equal-strength criterion are almost the same as those from the combined criterion of equal strength and efficient stress transfer up to the optimal level of hierarchy, at which the material simultaneously achieves equal strength and efficient stress transfer in the structure. Figure 4*d* suggests that the quasi-self-similar hierarchical material will not be able to remain flaw-tolerant beyond the optimal level. Generally, tougher soft matrices lead to higher material toughness and larger structure size with more hierarchical levels.

4. DISCUSSION

The results shown in figure 4 indicate that, depending on the mineral content, increasing the number of hierarchical levels tends to increase material toughness until the optimal level is reached; increasing the number of hierarchies beyond the optimal level leads to decreasing toughness. The reason for this behaviour is that structural hierarchy imposes two opposing effects on the material. First, it allows the stress and deformation to be optimally partitioned between the inclusions and matrix, leading to higher toughness. However, higher toughness comes at a cost of decreasing strength, making it increasingly difficult to drive the deformation of the soft matrix unless smaller and smaller inclusion aspect ratios are used (see electronic supplementary material, table S1). This leads to an upper limit in the achievable toughness. In general, materials with low levels of hierarchy have high strength but low toughness, while materials with high levels of hierarchy have low strength but high toughness. A balance is achieved at the optimal level of hierarchy.

Table 1 lists the size and mechanical properties of the quasi-self-similar material at different hierarchical levels for $\Theta_p = 35\%$ up to the optimal level $N = 4$. It can be seen that the characteristic size varies from tens of nanometres ($h_0 = 18$ nm for mineral bits at the bottom level) to hundreds of micrometres for the mineralized tendon fibre, and structural hierarchy becomes increasingly less effective in elevating toughness and structure size as the optimal level is reached. The predicted size scales and the optimal level of hierarchy are consistent with the experimental observations [18–20]. The magnification of toughness up to the optimal level is achieved at the cost of decreasing stiffness and strength at increasing hierarchical levels, which is consistent with the experimental observations [11,35,36].

Table 1. The predicted size and properties at different hierarchical levels of the mineralized tendon fibre based on the quasi-self-similar hierarchical model with $\Theta_p = 35\%$.

level n	h_n/h_0	h_n/h_{n-1}	ρ_n	l_n/l_{n-1}	E_n/E_m	S_n/σ_m	Γ_n/γ_m
0	1	—	7.14E + 01	—	1	1	2
1	2.42E + 01	24.2	2.22E + 01	7.52	4.22E − 01	2.22E − 01	5.66E + 00
2	3.81E + 02	15.7	6.91E + 00	4.90	8.54E − 02	6.91E − 02	4.26E + 01
3	2.24E + 03	5.90	2.15E + 00	1.84	9.96E − 03	2.15E − 02	2.09E + 02
4	4.26E + 03	1.90	—	—	9.96E − 04	6.69E − 03	3.83E + 02

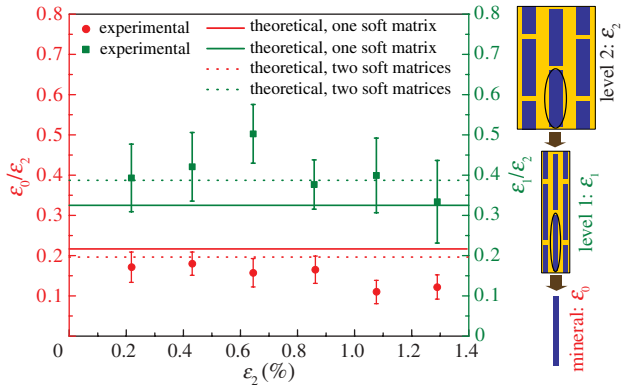

Figure 5. Plots of strain ratios $\varepsilon_0 : \varepsilon_2$ (red circles) and $\varepsilon_1 : \varepsilon_2$ (green squares) for the first three levels of hierarchy in mineralized tendon fibre against experimental data [11]. Error bars are standard errors of the mean. Solid lines, theoretical, one soft matrix; dotted lines, theoretical, two soft matrices.

Our model shows that the ratio between strains at adjacent hierarchical levels satisfies $\varepsilon_{n+1} : \varepsilon_n = (\varphi_n \sigma_n / E_{n+1}) : (\sigma_n / E_n) = \varphi_n (E_n : E_{n+1})$. Figure 5 plots the strain ratios $\varepsilon_0 : \varepsilon_2$ and $\varepsilon_1 : \varepsilon_2$ for the first three hierarchical levels against the corresponding experimental data measured by Gupta *et al.* [11]. Under the present assumption of an identical soft matrix at all hierarchical levels, our model predicts $\varepsilon_2 : \varepsilon_1 : \varepsilon_0 = 12 : 3.9 : 2.6$. In comparison, the experimentally measured strain ratios between tissue, fibril and mineral are $\varepsilon_2 : \varepsilon_1 : \varepsilon_0 = 12 : 5 : 2$ [11]. The agreement is reasonable considering that real biological materials have more than one type of soft materials. In fact, better agreement (12 : 4.6 : 2.4 versus 12 : 5 : 2) can be achieved as soon as two different types of soft matrix are taken into account, as shown in figure 5, without altering the optimal level number $N = 4$ (for details see electronic supplementary material, text B, figure S2 and table S2).

Calculations using mineral contents comparable to those in bone and shell have also been performed (see electronic supplementary material, text D, figures S4 and S5). Table 2 summarizes the parameters and the predicted optimal structures for bone, mineralized tendon and shell. It can be seen that the optimal level of hierarchy for bone is 4–6 if the fracture strain of soft matrix is taken to be $\Theta_p = 35$–100%, while experiments show that bone has seven levels of hierarchy [16,17]. This is deemed a reasonable agreement given that the structure of bone ceases to be self-similar beyond the bottom three levels. For shell, our analysis indicates that no hierarchical structure is necessary if the soft matrix fails at $\Theta_p = 35\%$ while four levels of structural hierarchy is optimal if more resilient soft matrix with $\Theta_p = 100\%$ is used. The predicted

Table 2. Predicted optimal levels of hierarchy versus experimental observations for various load-bearing biological materials.

		optimal N		N[b] observed in nature
	Φ (%)[a]	$\Theta_p = 35\%$	$\Theta_p = 100\%$	
bone	45	4	6	7
mineralized tendon	15	4	6	4–6
shell	95	1	4	2–3

[a]Jackson *et al.* [6], Jager & Fraatzl [7], Menig *et al.* [21] and Landis [34].
[b]Rho *et al.* [16], Weier & Wagner [17], Puxkandl *et al.* [18], Kastelic *et al.* [19] and Menig *et al.* [21].

1–4 levels of hierarchy are close to experimentally observed 2–3 levels in shells [21]. The predicted trend of decreasing number of hierarchical levels from bone to mineralized tendon and shell is in agreement with the experimental observations.

Our present analysis indicates that the previously developed hierarchical model [10,12] failed to explain experimentally observed behaviours of load-bearing biological materials because of the assumption of geometrical self-similarity, which implicitly demands a limitless selection of ever weaker soft materials at higher hierarchical levels. By contrast, nature is constrained by a very limited selection of structural proteins (primarily collagen). Our present model recognizes this fact and therefore correctly predicts the key experimental observations, including that there exists an optimal level of structural hierarchy.

It is worth pointing out that human beings have been able to discover and develop many materials, notably various metals, metallic alloys, ceramics, plastics, as well as their composites, with performances significantly surpassing biological materials [14]. However, it is not difficult to realize that most of the man-made materials are not environmentally friendly and have not been developed with genuine concerns over their sustainability on the evolutionary timescale. By contrast, biological materials are based on relatively weak constituents such as minerals and proteins which are easily degradable, bio-compatible, pollution-free, recyclable and energy-efficient. These properties are essential for long-term sustainability in evolution, and can be expected to become increasingly important to human civilizations as we approach the limit of natural resources. Understanding the hierarchical design principles of biological materials can provide useful guidelines on developing bioinspired 'green materials' based on bio-degradable and energy-efficient, hence environmentally friendly, materials in the future.

In summary, our work shows that the evolution of load-bearing biological materials may have been guided by a clear set of physical principles/rules. We have shown that the experimentally observed hierarchical structures in load-bearing biological materials can be understood based on a quasi-self-similar model of hierarchical composite material. In this model, we have adopted a number of design rules including flaw-tolerance, equal strength and efficient stress transfer, while recognizing the fact that there is only a limited selection of constituent materials in nature. Using typical parameters of biological materials, our analysis indicates that there exists an optimal number of hierarchical levels, hence an optimal hierarchical structure, for maximum material toughness. Within the optimal hierarchy, the characteristic size from the bottom to top structures varies from tens of nanometres to hundreds of micrometres. These predictions are all in agreement with the experimental observations. The ratio between strains at the bottom three levels of hierarchy shows quantitative agreement with the experimental measurements. The predicted trend of decreasing number of hierarchical levels from bone to mineralized tendon and shell is also consistent with experiments. Our model reveals a number of physical principles/rules for load-bearing biological materials, which may benefit the development of biomimetic 'green' materials that are not only endowed with superior mechanical properties but also biocompatible, degradable, environment-friendly and energy-efficient.

This work was supported by the A*STAR Visiting Investigator Program 'Size Effects in Small Scale Materials' hosted at the Institute of High Performance Computing in Singapore.

APPENDIX A. CRITICAL ASPECT RATIO FOR EFFICIENT STRESS TRANSFER

Efficient stress transfer plays a key role in all composite materials, and in particular depends on the aspect ratio of hard inclusions in biocomposites [30,31]. In the staggered composites, the soft protein matrix usually has relatively low Young's modulus and yield stress but large capacity of plastic deformation. In considering stress transfer, we model it as an ideal plastic material, as shown in figure 6. Equilibrium equations for hard inclusions 1 and 2 in figure 6 can be written as

$$\frac{\mathrm{d}u_1(x)}{\mathrm{d}x} = \frac{2\tau_n^p}{h_n E_n}\left(\frac{l_n}{2} - x\right) \tag{A 1}$$

and

$$\frac{\mathrm{d}u_2(x)}{\mathrm{d}x} = \frac{2\tau_n^p}{h_n E_n} x, \tag{A 2}$$

respectively.

Subtracting equation (A 1) from equation (A 2) yields

$$\frac{\mathrm{d}(u_2 - u_1)}{\mathrm{d}x} = \frac{2\tau_n^p}{h_n E_n}\left(2x - \frac{l_n}{2}\right). \tag{A 3}$$

The thickness of the soft matrix layer between neighbouring inclusions can be expressed in terms of the thickness h_n and volume fraction φ_n of hard inclusions as $(1-\varphi_n)h_n/\varphi_n$. Hence, shear deformation in the soft

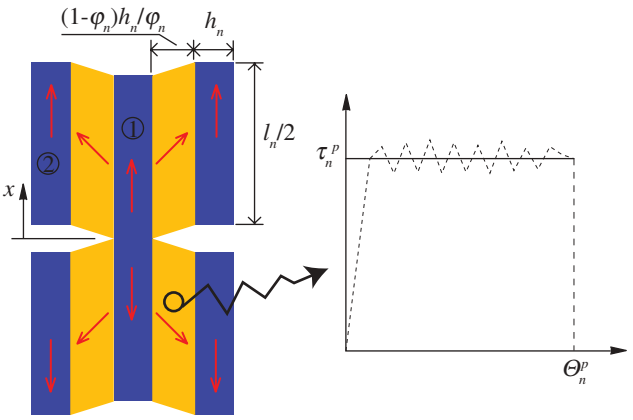

Figure 6. Stress transfer in the tension-chain model of biocomposites under uniaxial tensile load. The soft matrix (yellow) is modelled as an idealized plastic material. The dotted line depicts the general constitutive behaviour of protein.

layer can be derived by integrating equation (A 3),

$$\gamma(x) = \frac{\varphi_n(u_2 - u_1)}{(1-\varphi_n)h_n} = \frac{2\varphi_n\tau_n^p}{(1-\varphi_n)h_n^2 E_n}\left(x^2 - \frac{l_n}{2}x + C\right). \tag{A 4}$$

For efficient stress transfer, the following conditions must be satisfied:

$$\min\gamma = \frac{2\varphi_n\tau_n^p}{(1-\varphi_n)h_n^2 E_n}\left(-\frac{l_n^2}{16} + C\right) = 0, \quad \text{when } x = \frac{l_n}{4} \tag{A 5}$$

and

$$\max\gamma = \frac{2\varphi_n\tau_n^p}{(1-\varphi_n)h_n^2 E_n} \cdot C = \Theta_n^p, \quad \text{when } x = 0 \text{ or } \frac{l_n}{2}. \tag{A 6}$$

Combing equations (A 5) and (A 6), the critical length for efficient stress transfer is determined as

$$l_n^{\mathrm{STC}} = 2h_n\sqrt{\frac{2(1-\varphi_n)\Theta_n^p E_n}{\varphi_n\tau_n^p}}, \tag{A 7}$$

and consequently the critical aspect ratio as

$$\rho_n^{\mathrm{STC}} = 2\sqrt{\frac{2(1-\varphi_n)E_n}{\varphi_n\tau_n^p/\Theta_n^p}}. \tag{A 8}$$

Note that this result is based on a direct analysis of tension-shear structure and differs slightly from that of Chen *et al.* [31].

REFERENCES

1 Currey, J. D. 1984 *The mechanical adaptations of bones*. Princeton, NJ: Princeton University Press.
2 Neinhuis, C. & Barthlott, W. 1997 Characterization and distribution of water-repellent, self-cleaning plant surfaces. *Ann. Bot.* **79**, 667–677. (doi:10.1006/anbo.1997.0400)
3 Autumn, K., Liang, Y. A., Hsieh, S. T., Zesch, W., Chan, W. P., Kenny, T. W., Fearing, R. & Full, R. J. 2000 Adhesive force of a single gecko foot-hair. *Nature* **405**, 681–685. (doi:10.1038/35015073)

4 Fratzl, P. & Weinkamer, R. 2007 Nature's hierarchical materials. *Prog. Mat. Sci.* **52**, 1263–1334. (doi:10.1016/j.pmatsci.2007.06.001)
5 Fratzl, P. & Barth, F. G. 2009 Biomaterial systems for mechanosensing and actuation. *Nature* **462**, 442–448. (doi:10.1038/nature08603)
6 Jackson, A. P., Vincent, J. F. V. & Turner, R. M. 1988 The mechanical design of nacre. *Proc. R. Soc. Lond. B* **234**, 415–440. (doi:10.1098/rspb.1988.0056)
7 Jager, I. & Fratzl, P. 2000 Mineralized collagen fibrils: a mechanical model with a staggered arrangement of mineral particles. *Biophys. J.* **79**, 1737–1746. (doi:10.1016/S0006-3495(00)76426-5)
8 Gao, H. J., Ji, B. H., Jager, I. L., Arzt, E. & Fratzl, P. 2003 Materials become insensitive to flaws at nanoscale: lessons from nature. *Proc. Natl Acad. Sci. USA* **100**, 5597–5600. (doi:10.1073/pnas.0631609100)
9 Ji, B. H. & Gao, H. J. 2004 Mechanical properties of nanostructure of biological materials. *J. Mech. Phys. Solids* **52**, 1963–1990. (doi:10.1016/j.jmps.2004.03.006)
10 Gao, H. J. 2006 Application of fracture mechanics concepts to hierarchical biomechanics of bone and bone-like materials. *Int. J. Fract.* **138**, 101–137. (doi:10.1007/s10704-006-7156-4)
11 Gupta, H. S., Seto, J., Wagermaier, W., Zaslansky, P., Boesecke, P. & Fratzl, P. 2006 Cooperative deformation of mineral and collagen in bone at the nanoscale. *Proc. Natl Acad. Sci. USA* **103**, 17 741–17 746. (doi:10.1073/pnas.0604237103)
12 Yao, H. M. & Gao, H. J. 2007 Multi-scale cohesive laws in hierarchical materials. *Int. J. Solids Struct.* **44**, 8177–8193. (doi:10.1016/j.ijsolstr.2007.06.007)
13 Tang, Z., Kotov, N. A., Magonov, S. & Ozturk, B. 2003 Nanostructured artificial nacre. *Nat. Mat.* **2**, 413–418. (doi:10.1038/nmat906)
14 Bonderer, L. J., Studart, A. R. & Gauckler, L. J. 2008 Bioinspired design and assembly of platelet reinforced polymer films. *Science* **319**, 1069–1073. (doi:10.1126/science.1148726)
15 Munch, E., Launey, M. E., Alsem, D. H., Saiz, E., Tomsia, A. P. & Ritchie, R. O. 2008 Tough, bio-inspired hybrid materials. *Science* **322**, 1516–1520. (doi:10.1126/science.1164865)
16 Rho, J.-Y., Kuhn-Spearing, L. & Zioupos, P. 1998 Mechanical properties and the hierarchical structure of bone. *Med. Eng. Phys.* **20**, 92–102. (doi:10.1016/S1350-4533(98)00007-1)
17 Weiner, S. & Wagner, H. D. 1998 The material bone: structure mechanical function relations. *Annu. Rev. Mat. Sci.* **28**, 271–298. (doi:10.1146/annurev.matsci.28.1.271)
18 Puxkandl, R., Zizak, I., Paris, O., Keckes, J., Tesch, W., Bernstorff, S., Purslow, P. & Fratzl, P. 2002 Viscoelastic properties of collagen: synchrotron radiation investigations and structural model. *Phil. Trans. R. Soc. Lond. B* **357**, 191–197. (doi:10.1098/rstb.2001.1033)
19 Kastelic, J., Galeski, A. & Baer, E. 1978 The multicomposite structure of tendon. *Connect. Tissue Res.* **6**, 11–23. (doi:10.3109/03008207809152283)
20 Screen, H. R. C. 2009 Hierarchical approaches to understanding tendon mechanics. *J. Biomech. Sci. Eng.* **4**, 481–499. (doi:10.1299/jbse.4.481)
21 Menig, R., Meyers, M. H., Meyers, M. A. & Vecchio, K. S. 2001 Quasi-static and dynamic mechanical response of *Strombus gigas* (conch) shells. *Mat. Sci. Eng. A* **297**, 203–211.
22 Currey, J. D. 2009 Measurement of the mechanical properties of bone: a recent history. *Clin. Orthop. Relat. Res.* **467**, 1948–1954. (doi:10.1007/s11999-009-0784-z)
23 Su, Y. W., Ji, B. H., Zhang, K., Gao, H. J., Huang, Y. G. & Hwang, K. C. 2010 Nano to micro structural hierarchy is crucial for stable superhydrophobic and water-repellent surfaces. *Langmuir* **26**, 4984–4989. (doi:10.1021/la9036452)
24 Qin, Z., Cranford, S., Ackbarow, T. & Buehler, M. J. 2009 Robustness-strength performance of hierarchical alpha-helical protein filaments. *Int. J. Appl. Mech.* **1**, 85–112. (doi:10.1142/S1758825109000058)
25 Yao, H. M. & Gao, H. J. 2006 Mechanics of robust and releasable adhesion in biology: bottom-up designed hierarchical structures of gecko. *J. Mech. Phys. Solids* **54**, 1120–1146. (doi:10.1016/j.jmps.2006.01.002)
26 Gao, H. J. & Chen, S. H. 2005 Flaw tolerance in a thin strip under tension. *J. Appl. Mech.* **72**, 732–737. (doi:10.1115/1.1988348)
27 Taylor, D., Hazenberg, J. G. & Lee, T. C. 2007 Living with cracks: damage and repair in human bone. *Nat. Mat.* **6**, 263–268. (doi:10.1038/nmat1866)
28 Liu, B., Zhang, L. X. & Gao, H. J. 2006 Poisson ratio can play a crucial role in mechanical properties of biocomposites. *Mech. Mat.* **38**, 1128–1142. (doi:10.1016/j.mechmat.2006.02.002)
29 Cox, H. L. 1952 The elasticity and strength of paper and other fibrous materials. *Br. J. Appl. Phys.* **3**, 72–79. (doi:10.1088/0508-3443/3/3/302)
30 Buehler, M. J. 2006 Nature designs tough collagen: explaining the nanostructure of collagen fibrils. *Proc. Natl Acad. Sci. USA* **103**, 12 285–12 290. (doi:10.1073/pnas.0603216103)
31 Chen, B., Wu, P. D. & Gao, H. J. 2009 A characteristic length for stress transfer in the nanostructure of biological composites. *Comp. Sci. Technol.* **69**, 1160–1164. (doi:10.1016/j.compscitech.2009.02.012)
32 Termine, J. D. & Robey, P. G. (eds) 1996 *Primer on the metabolic bone diseases and disorders of mineral metabolism. An official publication of the American Society for Bone and Mineral Research*. New York, NY: Lippincott-Raven Publishers.
33 Fratzl, P., Gupta, H. S., Paschalis, E. P. & Roschger, P. 2004 Structure and mechanical quality of the collagen-mineral nano-composite in bone. *J. Mat. Chem.* **14**, 2115–2123. (doi:10.1039/b402005g)
34 Landis, W. J. 1995 The strength of a calcified tissue depends in part on the molecular structure and organization of its constituent mineral crystals in their organic matrix. *Bone* **16**, 533–544. (doi:10.1016/8756-3282(95)00076-P)
35 Gupta, H. S., Messmer, P., Roschger, P., Bernstorff, S., Klaushofer, K. & Fratzl, P. 2004 Synchrotron diffraction study of deformation mechanisms in mineralized tendon. *Phys. Rev. Lett.* **93**, 158101. (doi:10.1103/PhysRevLett.93.158101)
36 Gupta, H. S., Wagermaier, W., Zickler, G. A., Aroush, D. R. B., Funari, S. S., Roschger, P., Wagner, H. D. & Fratzl, P. 2005 Nanoscale deformation mechanisms in bone. *Nano Lett.* **5**, 2108–2111. (doi:10.1021/nl051584b)